# On Divergence-Angle Efficiency of a Laser Beam in Free-Space Optical Communications for High-Speed Trains

Yagiz Kaymak, *Student Member, IEEE,* Roberto Rojas-Cessa, *Senior Member, IEEE,* Jianghua Feng, Nirwan Ansari, *Fellow, IEEE,* Mengchu Zhou, *Fellow, IEEE*

***Abstract*—We first compare two different laser beam modalities, narrow and wide beam, in a free-space optical (FSO) communications system for ground-to-train high-speed train communications in which we analyze the trade-offs among receiving power, coverage area, and the complexity of the acquisition-tracking-pointing (ATP) mechanism. We then propose to employ a divergence angle of a wide beam in the range [0.07°, 2.002°] to relax the steering speed of the fast steering mirror (FSM), which is one of the major components of the ATP mechanism in an FSO transceiver. In addition, a beam using a divergence angle in the proposed range allows us to overcome the negative effects of vertical vibrations induced by the train's motion. The proposed range of divergence angles provides a large link range and effective coverage length and contact time as compared to a narrow beam.**

***Index Terms*—free-space optical communications, optical wireless communications, high-speed train communications, beam divergence angle, wide beam, narrow beam.**

## I. Introduction

HIGH-SPEED trains (HSTs), which travel at speeds of 300 km/h or faster, play an increasing role in public transportation as the number of passengers traveling in them increases. For example, the number of HST passengers in China has increased from 128 million in 2008 to 672 million in 2013, which represents an annual growth of approximately 39% during that period [1]. Because of the increasing number of passengers, the demand for high-speed Internet access on HSTs is also on the rise [2].

Several technologies are being considered for HST communications. Radio frequency (RF) wireless technologies are currently being used to provide Internet access to HST passengers [3]. Wireless fidelity (Wi-Fi), worldwide interoperability for microwave access (WiMAX), and leaky coaxial cables are employed to provide Internet access to HSTs in several countries, but they cannot provide high data rates due to interference, bandwidth limitations and the inherent limited data rates of RF technology [4]–[8]. Wi-Fi and WiMAX can potentially deliver peak data rates of up to 75 Mbps, but the actual data rates are lower than 10 Mbps [9].

Free-space optical (FSO) communication is an alternative approach. This is a line-of-sight technology that uses modulated light to transfer data through air, vacuum, or outer space [10]. An FSO communications system comprises three stages: a transmitter to send the optical signals, a free space transmission channel, and a receiver to acquire the transmitted signals. Each party (i.e., the transmitter and receiver) is usually equipped with a transceiver that functions as a transmitter and receiver at the same time to provide full duplex FSO communications. In the remainder of this paper, we assume that each party; a train and a ground base station (BS), is equipped with a transceiver. Laser diodes operating at wavelengths between 780 and 1600 nm are usually preferred as the light sources for this application because they may provide high data rates over long distances. For instance, FSO systems are expected to provide data rates in the range of Gigabits per second for HSTs [2], [11]. FSO systems also have additional benefits over RF technologies including immunity to electromagnetic interference and high security owing it to the use of directed light and of an unregulated range of the spectrum [3], [10].

Both parties in an FSO communications system must be aligned carefully to point the transmitting laser beam to the receiver [12]. Alignment is even needed for stationary transceivers. For example, building-to-building FSO communications use alignment and tracking mechanisms to handle the motion of transceivers generated by thermal expansion, wind sway, and vibration [12]. This alignment mechanism is usually called acquisition-tracking-pointing (ATP) [13]. The alignment of the beam and receiver becomes challenging when the transmitter, receiver, or both parties are in motion. The extent of impairing effects, such as vibration, is expected to be severe in ground-to-train FSO communications for HSTs. In this context, an ATP mechanism is used to acquire the exact location of the ground/train transmitter/receiver (in both parties), point the transmitter to the receiver, and correct the pointing/tracking errors while the train is in motion [14].

As all other communication technologies proposed to provide Internet access to HSTs, transceivers must be able perform handovers for continuous communication along the track while the train travels. Handover is defined as the process of transferring an ongoing call/data session from one (i.e., source) BS to another (i.e., target) BS when a mobile node travels from



Y. Kaymak, R. Rojas-Cessa, Nirwan Ansari, and Mengchu Zhou are with the Networking Research Laboratory, Department of Electrical and Computer Engineering, New Jersey Institute of Technology, Newark, NJ 07102. Email: {yk79, rojas, nirwan.ansari, zhou}@njit.edu.

Jianghua Feng is with CSR Zhuzhou Institute Co., LtD, Shidai Road, Zhuzhou, Hunan Province, China Email: fengjh@csrzic.com.

Manuscript received XXX, XX, 2016; revised XXX, XX, 2017.

the coverage area of the source BS to the coverage area of the target BS [15]. Handover in RF communications systems, such as long-term evolution (LTE), IEEE 802.11p, WiMAX, and Radio-over-fiber (RoF), is performed based on measurements of the channel quality, such as the received signal strength (RSS), signal to interface ratio (SIR), and the bit error rate (BER), over an overlapping region covered by two or more adjacent BSes [16]–[18]. When the channel quality indicator of the link between the mobile node and a BS drops below a pre-determined threshold, handover is carried out from the source BS to target BS.

Handover in FSO may be handled in a different way from a handover in RF communications systems because of the light beam characteristics as compared to the omnidirectional transmission in RF. A part of the handover process in FSO involves the alignment of a fast steering mirror (FSM), which is used to align the transmitter to the receiver. The alignment mechanism steers the mirror from source BS to target BS as the mobile node enters the coverage area of the target BS [2], [11]. For HSTs, handover is performed frequently and it may shorten the connection time, which is the time when the train's transceiver transmits and receives user data [11]. Another handover-related problem for FSO in HSTs is the steering speed of the FSM used in FSO transceivers. The angular steering speed of the FSM for a train moving at high speed may not be satisfied by off-the-shelf FSMs [19]–[21]. Moreover, the train-induced vibration can make the connection unstable and delay or hinder the handover process [22].

FSO beams for optical wireless communications can be categorized into two modalities: narrow and wide beams. An FSO beam with a divergence angle smaller than or equal to 0.0057° is considered to be a narrow beam, and, therefore, a beam with a larger divergence angle is considered to be a wide one [12], [23]–[25].

The narrow and highly collimated characteristics of a laser beam make ground-to-train FSO communications challenging. Specifically, a narrow beam can generate larger pointing/tracking errors than a wide beam because of environmental disturbances such as the vibration induced by a train's motion, track irregularities, and the turbulence effect generated by a train moving through the atmosphere. Vibrations can cause a significant reduction in the amount of received power at the receiver, resulting in transmission errors [26]. The train vibrations increase detector decoupling loss, which is defined as the ratio of the optical power in the receiver's focal plane to the power incident on the active area of the optical detector [12]. As the received beam spot wanders off the center of the optical detector, the detector coupling loss increases and the received power decreases. Among the types of train vibrations (i.e., vertical, lateral and longitudinal) vertical vibrations generate the largest displacement of the train (and transceivers) [27]. Therefore, we focus on vertical vibrations and their impact on received power. The use of a narrow beam requires a precise alignment if the narrow-laser-based link operates over a long range, such as 1 km [28], [29]. Such a precise alignment requirement may jeopardize the connectivity between the two parties [30]. Therefore, it is clear that an ATP mechanism is required for narrow FSO beams to track the train and ensure alignment.

Feedback control mechanisms may be used in FSO communications systems as a part of the ATP subsystem to mitigate the effects of vibration and pointing errors that might be induced by the motion of the transmitter, the receiver, or both [2], [11], [31]–[33]. Measurements from position-sensing detectors, quadrant photodiodes (QPDs), or complementary metal-oxide-semiconductor (CMOS) sensors may be used to control and align the transceiver. Moreover, wide-angle beacon lights might be employed as a part of the ATP mechanism to align the transceivers [2], [11].

A wide beam may generate a large spot size at the receiver location to cover the transceiver or even the complete train car. Therefore, the use of a wide beam may relax the constraints on an ATP mechanism, such as the steering speed of the FSM, or completely eliminate the need for an ATP [34]. On the other hand, a narrow beam may require a faster FSM steering speed.

In this paper, we employ a geometrical model to represent a ground-to-train FSO communications system and to analyze its performance. Using this geometrical model, we present a comparison between the two beam modalities. This work aims to reveal which of the beam modalities lowers the complexity of an FSO communications system. In addition, we propose a range of beam divergence angles, [0.07°, 2.002°], that is selected according to practical constrains, such as the maximum speed of a fast steering mirror to track a high-speed train at 300 km/h, the connection time between the train and a BS, and the trains vertical displacements of up to 60 mm. The smallest divergence angle in the proposed range, 0.07°, is selected to keep the needed angular speed of a commercial FSM [19]. This maximum angular speed dictates the minimum divergence angle of the proposed range when the tilt angle of the beam is 45° or larger. The largest divergence angle in the proposed range, 2.002°, is selected to allow a connection time of at least twice the largest handover time, which is reported as 1 second for an FSO communications systems for high-speed trains (HSTs) [22]. Moreover, all divergence angles in the proposed range mitigate the impairing effect of the vibration induced by the motion of the train without resorting to a feedback-control mechanism while guaranteeing high data rates (1 Gbps or higher). Furthermore, to the best of our knowledge, this is the first work that compares narrow and wide beam modalities used in FSO communications for HSTs.

The remainder of the paper is organized as follows. Section II summarizes the related work. Section III presents our geometrical system model. Section IV compares the narrow and the wide beam modalities and lists the advantages and disadvantages of each modality in FSO communications for HSTs. Section V presents our results. Section VI concludes the paper.

## II. Related Work

A high data-rate ground-to-train FSO communications system was proposed and implemented by using a laser beam with a divergence angle of 0.29° operating at a wavelength of 750 nm [11]. The proposed FSO communications system

employs an ATP mechanism for performing tracking and handover. A light emitting diode (LED) beacon with wide-beam characteristics is used for coarse tracking and handover, and a narrow laser beam is used for fine tracking and the actual data transmission [11]. Moreover, an FSM and two QPDs are employed as a part of the ATP mechanism. These two QPDs, one with a wide-angle lens and the other one with a telescopic (i.e., narrow) lens, are both used to adjust the mirror's angle [11]. In the same work, a beacon-light-assisted handover is proposed. Beacon lights are used to inform other transceivers about its presence. Lenses placed in front of the QPDs focus the beacon lights on the QPDs that control the FSM to align the transmitting laser to the target BS according to the light intensity differences on the quadrants of the QPDs in case of a handover. An overlapping region illuminated by the source and the target BSes allows the transceiver on the train to capture two beacon lights and to switch from the source BS to the target BS during the handover.

In another version of an ATP, the wide-angle lens is replaced by a high-speed image sensor that can detect the actual position of the beacon light faster than a QPD [2]. This image sensor allows high-speed detection and acquisition of the beacon light emitted from the target BS and decreases the total handover time by providing a more precise position of the target BS than a QPD.

A geometric model employing a wide beam with a divergence angle of 3.2° was introduced for high-speed ground-to-train FSO communications [3], [35]. However, this work misses to compare different beam modalities. We adopt this geometric model to compare and analyze different beam modalities.

A dual-link approach may use a wide and narrow LED beam at the same time for outdoor FSO communications [36]. The wide beam acts as a robust link that provides acquisition and alignment support for the narrow beam, which is used to deliver high data rates. The relaxed alignment constraints of the wide beam are well suited for mobile networks, such as high-speed ground-to-train FSO communications system. In this approach LEDs are used as the light sources, however, they may not be suitable for high data rates, i.e., 1 Gbps or higher, communications in HST because of their very large divergence angles [37]. Because the impact of vibration on the received power in HST has not been considered, we discuss it in this paper.

## III. System Model

We adopt a geometrical model [3] to compare and analyze the different beam modalities. The beam propagation model of the laser light considered in this paper is characterized as a Gaussian distribution [38], [39]. A Gaussian beam model is adopted in our analysis because it is a natural consequence of the laser resonant cavity, which has been widely adopted in the literature [12], [38].

In a typical ground-to-train FSO communications model, a train car has an FSO transceiver installed on the roof, and each BS on the ground has an FSO transceiver. Section V discusses the separation distance between two consecutive

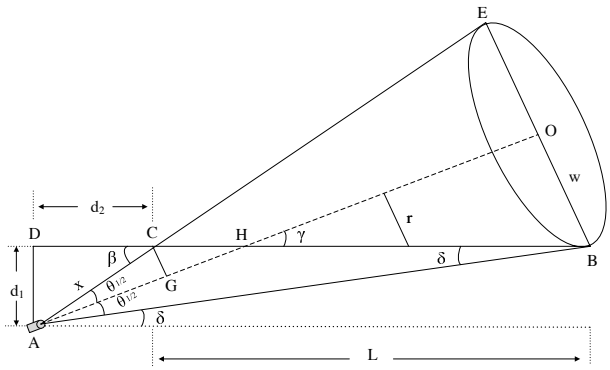


Fig. 1. Top view of the geometrical model of the ground-to-train FSO communications system along a straight track [DB].

BSes. For the sake of description, we focus on ground-to-train communications in this paper. Note that the establishment of a ground-to-train communications link also guarantees a train-to-ground link because the transmitter and receiver of a transceiver are aligned with the same orientation [11]. Therefore, our analysis actually applies to both links.

We consider that the transceiver on the train and the BSes along the track use a wavelength of 850 nm, which is denoted as $\lambda$. The 850-nm wavelength is selected because of its availability, reliability, high-performance capabilities, and the lower cost of the transmitter and detector [10]. We also consider that the transceiver of each BS might be connected to the fiber-optic backbone where a wavelength between 1530 and 1565 nm (i.e., C-band) is usually employed [40]–[42]. Owing to the different wavelengths that the proposed FSO communications system and a fiber-optic backbone operate, a fiber-to-fiber media converter [43]–[45] may be needed for wavelength conversion. Discussion on wavelength conversion is beyond the scope of this paper.

Figure 1 shows the geometrical model of the ground-to-train FSO communications system from a superior view (i.e., as seen from the top). In this figure, we assume that the train travels along line segment $[DB]$ from $D$ to $B$. $d_1$ denotes the distance between the BS and the track and is set to 1 m [3]. $d_2$ is the horizontal distance between the BS and the track and it designates the location of the shortest coverage point (represented by $C$) of the beam on the track. $\theta$ is the divergence angle of the laser beam. This angle impacts the beam radius, $w$, and the coverage length, $L$, along the track. In Figure 1, $tan\,\beta$ and $tan\,\delta$ are calculated as $tan\,\beta = d_1/d_2$ and $tan\,\delta = d_1/(d_2+L)$ using the triangles $ACD$ and $ABD$, respectively. Furthermore, because $\theta = \beta - \delta$, the coverage length of the light beam, $L$, in terms of $d_1$, $d_2$, and, $\theta$ can be represented as

$$L = \frac{x^2\, tan\,\theta}{d_1 - d_2\, tan\,\theta} \tag{1}$$

where $x$ is the hypotenuse of the triangle $ACD$ in Figure 1, and $x = \sqrt{{d_1}^2 + {d_2}^2}$. Denote $\theta_{1/2}$ as half of the divergence angle (i.e., $\theta_{1/2} = \frac{\theta}{2}$) and $\gamma = \theta_{1/2} + \delta$ as the tilt angle of the beam. The tilt angle is the angle between the optical axis

of the beam and the horizontal axis, which is parallel to the track. This angle affects $L$ because $\gamma$ is a function of $\delta$ and $\theta$. Note that $d_2$ affects the tilt angle of the transceiver on the ground. If $d_1$ is kept constant, the tilt angle of the laser beam decreases as $d_2$ increases. The height of the BS is the same as the height of the train, which is approximately about four meters above the ground level. $\overline{AO}$ in Figure 1 is the optical axis of propagation, and $z$ is the distance from the light source along the optical axis. The beam radius at distance $z$ is denoted by $w(z)$ and, is calculated by [38]:

$$w(z) = w_0 \sqrt{1 + \left(\frac{\lambda z}{\pi {w_0}^2}\right)^2}, \tag{2}$$

where $w_0 = \frac{\lambda}{\pi\, \theta_{1/2}}$ is the beam waist of the laser source at the transmitter. Here, $z = |AH| + |HO|$ and $|AH| = |AG| + |GH|$. In addition, the length of the line segment $[HO]$ can be written as $|HO| = (L - |CH|)\, cos\, \gamma$. Thus, $z$ can be given as $z = |AG| + |GH| + (L - |CH|)\, cos\, \gamma$. Therefore, $z$ can be written as:

$$z = L\, cos\, \gamma + x\, cos\, \theta_{1/2}, \tag{3}$$

where $r$ is the orthogonal offset from the optical axis of propagation of the light beam, which corresponds to the shortest distance between the $[GO]$ and $[CB]$ segments at distance $z$. For instance, $r$ is equal to $|CG|$ at the shortest coverage point $C$, and it is equal to $w(z)$ when $z$ is equal to $|AO|$. Considering triangle $OHB$, we obtain $r = (L - |CH|) sin\, \gamma$. Using a calculation similar to that in (3), $r$ is given as:

$$r = L\, sin\, \gamma - x\, sin\, \theta_{1/2}. \tag{4}$$

The received power at distance $z$ along the track for a Gaussian beam is [38]

$$P_{rx} = \frac{2\, P_{tx}\, A_c}{\pi\, (w(z))^2} e^{-(2r^2/(w(z))^2)}, \tag{5}$$

where $P_{tx}$ is the transmission power, and $A_c$ is the effective light collection area of the receiver. $A_c$ is given by [46]:

$$A_c = \frac{n^2\, A_d}{sin^2\, \psi_c}, \tag{6}$$

where $n$ is the refractive index of an optical concentrator that focuses the incoming light on the photodiode, in the receiver, $A_d$ is the photosensitive area of the photodiode in $m^2$, and $\psi_c$ is the half-angle field-of-view (FOV) of the receiver after the lens. For the analysis in Section V, we use $A_d = 7mm^2$, $\psi_c = 5.15°$, and $n = 1.5$ [3].

## IV. Comparison of The Narrow and Wide Beams

In this section, we compare the narrow and wide beam modalities of laser light transmission for high-speed ground-to-train FSO communications in HSTs. We discuss their strengths and weaknesses for HST communications.

FSO communications are susceptible to weather conditions such as fog, haze, rain, snow, and combinations of them [12]. In free space, these weather conditions may cause the atmospheric attenuation of the transmitted optical beam. Fog and haze cause the most severe attenuation because of the occurrence of Mie scattering in the wavelength band of interest (between 500 and 2000 nm) [10], [47]. A narrow beam has an advantage over a wide beam under bad weather conditions. Because decreasing the beam divergence decreases the spreading of the transmitted beam between the transmitter and the receiver, which in turn improves the link margin [3], [12]. Moreover, a higher link margin leads to an increase in the link range (i.e., the maximum achievable distance) for a given sensitivity of the receiver and makes a narrow beam preferred over a wide beam when the link range is considered [12]. As a consequence of the increase in the link range of a narrow beam, the separation distance between two consecutive BSes may be increased. Therefore, the total number of BSes along the track and their total cost may be smaller for a narrow-beam system than for a wide-beam system.

The light intensity of a narrow beam is greater than that of a wide beam at a given distance for sources with the same transmission power [26]. On the other hand, a narrow beam provides a shorter coverage length than a wide beam for a given tilt angle as (1) shows. Moreover, it is easier to block the light of a narrow beam than that of a wide beam. Therefore, some FSO products use multiple parallel beams to increase the reliability of the FSO link. If any of the parallel beams is blocked the unblocked beams can continue to communicate. For instance, a commercial FSO product uses 4 parallel beams that start overlapping at 100 meters [48]. If these parallel beams have large divergence angles, the combined coverage area of them is larger than that generated by multiple narrow beams, which may increase the reliability of FSO communications system.

Train vibrations generate larger pointing and tracking errors for a narrow beam than for a wide beam in high-speed ground-to-train FSO communications systems. Because the size of the receiver aperture of an FSO transceiver is usually small, train vibrations may cause the transmitting light to fall off of the receiver's aperture and this loss of line-of-sight may disrupt the connectivity between the BS and the train. Therefore, an ATP mechanism for a narrow beam is required to maintain the transmitter and the receiver of the FSO link aligned at all times, even in the occurrence of vibration induced by the motion of the train. The employment of such an ATP mechanism increases the cost of the FSO communications system [14].

Regarding security, it is harder to intercept a narrow beam than a wide beam because the narrow beam has a smaller spatial footprint and is highly directional. Furthermore, regardless of whether the beam is narrow or wide, laser light employed in FSO communications cannot penetrate walls or opaque obstacles, thus making eavesdropping difficult. Table I presents a comparison of the the properties, advantages and disadvantages of two beam modalities for high-speed ground-to-train FSO communications.

## V. Results and Discussion

In this section, we analyze and compare the two narrow- and wide- beam modalities in terms of the impact of the

TABLE I
COMPARISON OF NARROW AND WIDE BEAM

| Condition/Scenario | Preferred beam | Reason |
|---|---|---|
| Susceptibility to weather | Narrow | Using a narrow beam improves the link margin, which provides the system a greater chance to overcome adverse weather conditions such as fog, rain and snow [12]. |
| Maximum achievable distance | Narrow | Because the link margin is improved when a narrow beam is employed, a longer link range is provided with a narrow beam as compared to a wide beam at the receiver sensitivity threshold [12]. |
| Cost induced by the number of ground stations needed | Narrow | Because the maximum achievable distance is larger for a narrow beam, the total number of ground stations required and the cost incurred by the number of ground stations is smaller. |
| Light intensity | Narrow | A wide beam expands more with distance as compared to a narrow beam, which, in turn, causes the intensity of a wide beam to be less than that of a narrow beam at the same distance [26]. |
| Coverage length | Wide | The coverage length of a wide beam is larger than that of a narrow beam at the same distance from the transmitter with the same tilt angle. Our results support this fact. |
| Likelihood of blocking laser light | Wide | Because a narrow beam has a smaller spot size than that of a wide beam for the same distance, opaque objects are more likely to block the narrow beam than a wide beam. |
| Multiple parallel beams | Wide | Some commercial FSO products use multiple overlapping beams operating simultaneously to increase the reliability of the FSO link [48]. Overlapping wide laser beams at the receiver have a greater potential to increase the total coverage area than a narrow beam. Moreover, wider overlapping beams cannot be easily interrupted by obstacles between the transmitter and the receiver. |
| Vibration | Wide | Because the aperture size of the receiver is small (usually between 1-40 cm [49]), vibrations may cause pointing/tracking errors, if a narrow beam is used. If the pointing/tracking error induced by vibration is larger than the aperture size, connectivity may be jeopardized. |
| ATP requirement | Wide | An active ATP mechanism is required to maintain the link connectivity if a narrow beam is used [14]. However, using a wide beam may relax or eliminate this requirement. |
| Transceiver cost | Wide | ATP hardware increases the cost of the FSO system. Therefore, a narrow-beam system may be costlier than a wide-beam system [14]. |
| Security | Narrow | A narrow beam offers increased link security as the spatial footprint is small [50]. |

divergence angle of a laser beam on the maximum achievable distance (i.e., link range), coverage length, and contact time. We present the received power over different tilt angles and $d_2$ values. We analyze the angular speed of the FSM for various divergence angles and present the impact of train vibrations on the received power. We also report a laser experiment performed in a laboratory environment which shows the theoretical received power values in (5) match actual power values. The experimental results are provided at the end of this section.

Based on the results given in this section, we propose to employ a divergence angle of a wide beam in the range [0.07°, 2.002°] to drastically reduce the steering speed of the FSM, to accommodate vertical displacements of the train of up to 50 mm while guaranteeing a 1-Gbps data rate, and to provide connection time to the train that is larger than or equal to the handover time.

We use MATLAB® [51] to perform numerical evaluations of the models described from (1) to (6). We consider ON–OFF keying (OOK) as the adopted modulation scheme, which is widely used in FSO communications [12], [26]. A BER of $10^{-9}$ is adopted to guarantee an error-free data transmission for 1 Gbps at the receiver sensitivity threshold and no forward error coding scheme is used. We summarize the system model parameters used in the analysis of our FSO communications system in Table II.

According to (5), Figure 2 shows the maximum achievable distance along the track when $\theta$ varies from 0.002 to 3.002° in 0.1° steps; the maximum achievable distance for each $\theta$ is calculated according to the receiver sensitivity threshold, which is -36 dBm at 1 Gbps. The maximum achievable distance corresponds to the maximum distance at which the received light signal can be decoded and converted back to an electrical signal. We adopt -36 dBm as the receiver sensitivity threshold because silicon positive-intrinsic-negative (PIN) photodiodes with a transimpedance amplifier can provide data rates up to 1 Gbps at that sensitivity threshold by using an 850-nm laser [12], [24]. Also note that there are numerous FSO communications systems that provide a data rate of 1 Gbps or higher [12], [46], [52]–[56]. For instance, a fabricated indoor optical wireless communication system capable of transmitting at a line rate of 1.25 Gbps using an 825-nm-wavelength with a transmission power of 25 mW has been demonstrated [46]. This transmission power is slightly higher (i.e., 10 mW more) than the one used in our analysis [46], [53]. The same study shows that the measured sensitivity of the employed avalanche photodiode is -35 dBm at 1.25

TABLE II
SYSTEM MODEL PARAMETERS

| Symbol | Parameter | Value | Unit |
|---|---|---|---|
| $\theta$ | Beam divergence angle | variable | degree |
| $\lambda$ | Laser operating wavelength | 850 | nm |
| $\gamma$ | Tilt angle of the BS | variable | degree |
| $d_1$ | Vertical distance of the BS from the track | 1 | m |
| $d_2$ | Horizontal distance of the BS from the track | variable | m |
| $L$ | Coverage length of the beam | variable | m |
| $P_{tx}$ | Transmission power of the laser | 15 | mW |
| $S$ | Receiver sensitivity (at 1 Gbps) | -36 | dBm |
| $n$ | Refractive index of the optical concentrator | 1.5 | - |
| $\psi_c$ | Receiver half-angle field-of-view | 5.15 | degree |
| $A_d$ | Photo detector area | 7 | $mm^2$ |
| $f$ | Frequency of the vibration | 80 | Hz |
| $a$ | Amplitude of the vibration | [0, 60] | mm |
| $v$ | Speed of the train | 300 | km/h |

Gbps for a BER below $10^{-9}$. Moreover, commercial full duplex FSO communications products are reported to achieve data rates up to 1.25 Gbps with a range of up to 4 km in clear weather conditions [24]. Besides, 850-nm vertical-cavity surface-emitting lasers (VCSELs), usually employed in FSO communications systems, can be easily modulated at 2.5 GHz to provide a data rate of 2.5 Gbps, with a potential transmission capability of up to 10 Gbps [12], [52]. These approaches have been used in stationary and fixed BSes.

According to the results in Figure 2, the narrow beam reaches up to 181,696 meters from the BS while still providing enough (i.e., larger than the minimum receiver threshold) power. This result is expected because the highly collimated characteristics of the narrow laser beam lead to a significant increase in the intensity of the light at the receiver for a given transmitted power, which in turn results in a link range longer than that of a wide beam [26].

Based on the selected divergence angle, the maximum achievable distance of the beam determines the largest separation distance between two consecutive BSes. Therefore, each divergence angle in the proposed range is associated with a maximum achievable distance.

**Coverage Length.** According to (1), (5), and the receiver sensitivity threshold, Figure 2 shows the effective coverage length along the track when $\theta$ varies from 0.002 to 3.002° in 0.1° steps. As Figure 2 shows, with the increase in the maximum achievable distance, the effective coverage length of the narrow beam along the track increases.

**Contact Time.** Another metric is the contact time, which is defined as the time the transceivers are within the coverage area and eligible for establishing communication. The contact time includes the connection time and the time to perform handover. Figure 2 shows the contact time as $\theta$ varies from 0.002 to 3.002° in 0.1° for a HST moving at 300 km/h (or $83\frac{1}{3}$ m/s). The y-axis on the right of Figure 2 shows the contact time in seconds. As expected, the narrow beam provides the longest contact time because it attains the longest link range among the considered divergence angles. Table III summarizes the maximum achievable distances, effective coverage lengths along the track and contact times at 300 km/h for sampled $\theta$ values.

We use the largest divergence angle that allows a connection time of at least twice the handover time [22]. The largest reported handover time for FSO communications systems in HSTs is 1 second [22]. Considering that, a wide beam with a divergence angle smaller than or equal to 2.002° yields a contact time larger than 2 seconds, allowing a connection time of 1 second or longer (see Table III).

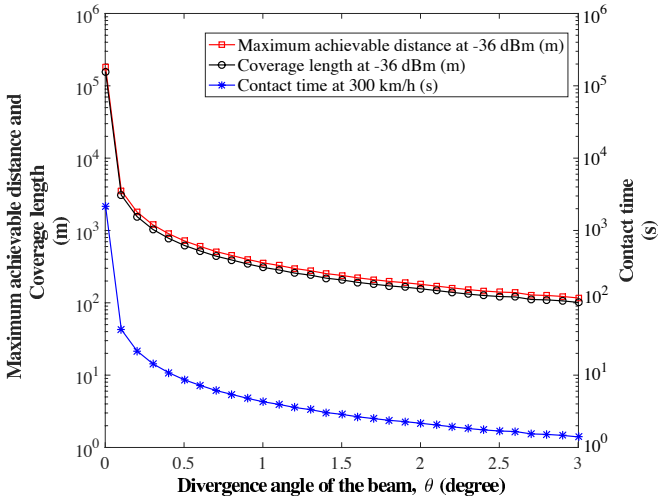


Fig. 2. The maximum achievable distance at -36 dBm (m), the coverage length at -36 dBm (m), and the contact time at 300 km/h (s) for $\theta$ from 0.002 to 3.002° in 0.1° steps.

**Received Power.** We graph the received power considering the receiver sensitivity threshold, tilt angle, and (5), as Figure 3 shows, when $\gamma$ decreases from 0.1 to 45.1°. The results in Figure 3 reveal that if the tilt angle for any of the considered wide beams is around 0°, the received power is not strong enough to allow the light be converted to an electrical signal for a data rate of 1 Gbps. On the other hand, the narrow beam provides a constant received power of approximately 20 dBm even if it is tilted more than 44.5°. Note that an increase in the tilt angle increases the achievable distance between the BS and the train, and the narrow beam has a considerably longer link range than a wide beam.

Figure 4 shows the received power when $d_2$ varies between 1 and 100 m, according to the sensitivity threshold and (5). This figure also shows that $d_2$ can reach beyond 100 meters

TABLE III
MAXIMUM ACHIEVABLE DISTANCE, EFFECTIVE COVERAGE LENGTH AND CONTACT TIME AT 300 KM/H FOR SAMPLED $\theta$ VALUES.

| $\theta$ (degrees) | Max Achievable Distance (m) | Effective Coverage Length (m) | Contact Time at 300 km/h (s) |
|---|---|---|---|
| 0.002 | 181,696 | 156,951 | 2,180 |
| 0.07 | 5,190 | 4,487 | 53.80 |
| 0.502 | 718.22 | 620.72 | 8.61 |
| 1.002 | 357.03 | 308.73 | 4.28 |
| 1.502 | 238.75 | 206.85 | 2.86 |
| 2.002 | 180.08 | 156.38 | 2.16 |
| 2.502 | 140.84 | 122.14 | 1.69 |
| 3.002 | 116.56 | 101.16 | 1.39 |

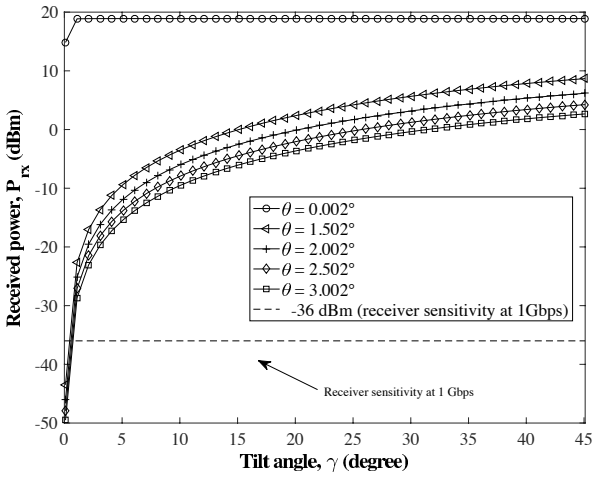


Fig. 3. Received power as a function of $\gamma$.

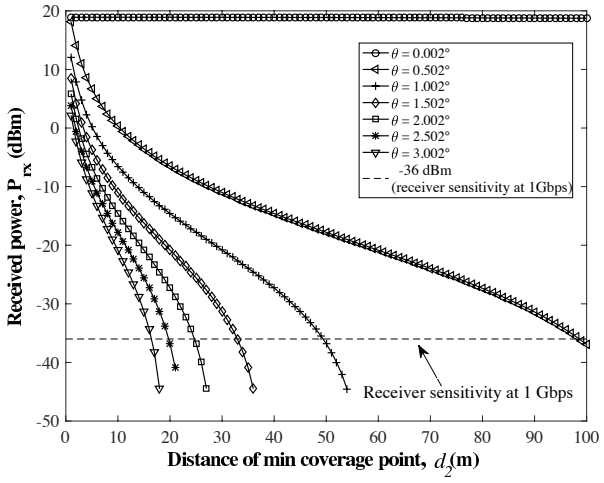


Fig. 4. Received power as the distance of the minimum coverage point varies between 1 m and 100 m.

without a significant decrease in power for the narrow beam. These results also show that a beam with a divergence angle in the proposed range may deliver enough power at the receiver to operate above the sensitivity threshold as $d_2$ approaches 100 m. Similar to the results shown in Figure 3, $d_2$ increases for a constant $d_1$ as the tilt angle decreases. Therefore, the horizontal distance between the BS and the track of the narrow beam is longer than that of the wide beam case.

An FSO transceiver is usually equipped with an optical concentrator, a photodiode and receiver electronics. The optical concentrator focuses the incident light onto the photodiode, whereas the photodiode converts the received light into electrical signals, which are then recovered by the receiver electronics. According to (5) and (6), an increase in the photosensitive area of the photodiode ($A_d$) or a decrease in the FOV of the concentrator (half of FOV angle is denoted as $\psi_c$) results in an increase in the received power ($P_{rx}$). The impact of $A_d$ on $P_{rx}$ is a direct result of the constant radiance theorem, which impacts the maximum collection area of an optical receiver for a given FOV, the reflective index of the optical concentrator, and the radiation collection area of the photodiode [46], [57]. Moreover, FOV has an adverse effect on the received power because the constant concentrator gain within the FOV of the optical concentrator (i.e., $\frac{n^2}{sin^2\,\psi_c}$) decreases when the FOV increases [3], [58], [59]. On the other hand, increasing the photosensitive area increases its capacitance and, therefore, decreases the response time of the diode [60]. Also, an increase of $A_d$ leads to a decrease of the receiver bandwidth and to contribute to the dark current noise of the photodiode in the absence of light [58]. In addition, an increase in FOV increases background noise, which degrades the signal-to-noise ratio of the received signal [61].

Figure 5 shows the relationship among $A_d$, $\psi_c$, and $P_{rx}$ for $\theta = 0.502°$. In this figure, $\theta$ is selected to show the impact of $A_d$ and $\psi_c$ on the received power when an arbitrary wide beam is selected from the divergence-angle range. In fact, any other divergence angle may also yield a similar graph. $A_d$ in this figure is selected in the commercially-available range of [0.1, 10] $mm^2$ [62]. We select the range of $\psi_c$ between 0.1 and

45° because the FOV of a concentrator is usually bound to 45° [58]. Figure 5 shows that a small FOV and large photosensitive area are beneficial to FSO communications systems because they yield a greater received power. The shaded zone of the 3D graph in this figure represents the $A_d$-$\psi_c$ pairs forming a region where the received power is at least -36 dBm for a data rate of 1 Gbps.

There are commercial large-area photodetectors operating at 10 Gbps or higher speeds, supporting the aforementioned relation between the size of the photosensitive area of a photodiode and its achievable data rate [63]–[66]. For instance, a receiver-optical subassembly (ROSA) InGaAs PIN photodiode with a preamplifier may provide a data rate of up to 11.3 Gbps with a photosensitive area of 1.25 mm [67]. Moreover, these ROSA modules may increase their received data rate up to 100 Gbps by employing WDM techniques [63]. These works show that photodiode areas larger than that considered in this paper may achieve larger data rates. However, this discussion is out of scope of this paper.

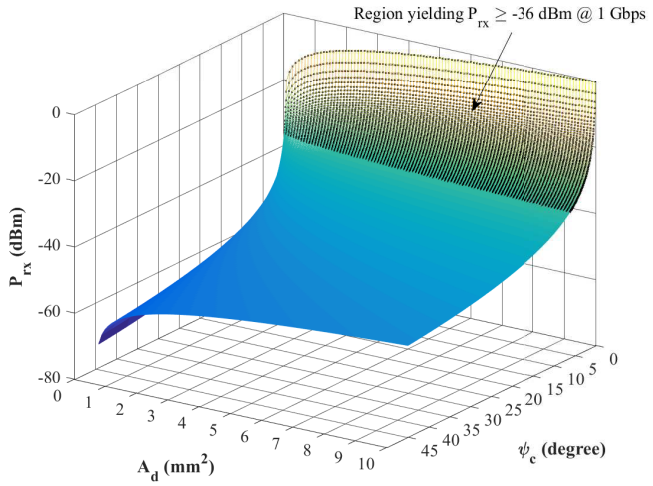


Fig. 5. Received power as a function of half-angle field-of-view and the size of the photosensitive area of the photodiode when $\theta$ = 0.502°.

**Angular Speed of FSM.** Figure 6 shows the angular speed of the FSM of a transceiver for a train moving at 300 km/h. The dashed line in this figure represents the maximum angular speed that a commercial FSM can reach, which equals to 300 radian/s, or 17188°/s [19]. In this calculation, we steer the FSM from 0.1 to 45.1° in 1° steps. For each $\{\theta, \gamma\}$ pair, we calculate the effective coverage length, $L_{\theta,\gamma}$, where $\theta$ and $\gamma$ are selected from the represented divergence and tilt angles, respectively. We obtain the required angular speed of the FSM by estimating the time it takes for the train to travel over each $L_{\theta,\gamma}$. Note that the speed of the FSM slows down as the beam divergence angle increases because the coverage length of a wide beam provides a longer contact time than that of the narrow beam. Figure 6 shows that the maximum angular speed of the narrow beam is required to be approximately 598,935 degree/s. However, this speed is infeasible for commercially available FSMs [19]–[21].

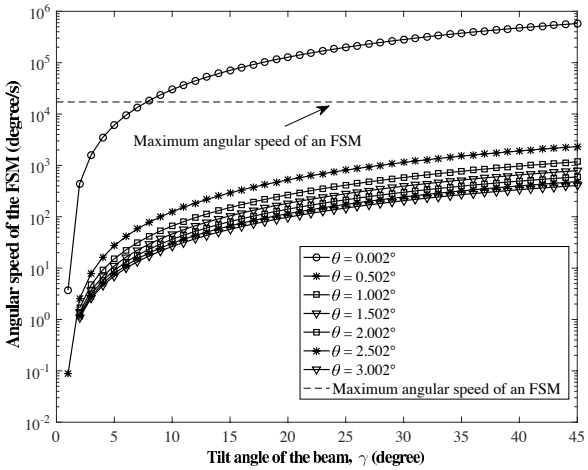


Fig. 6. Angular speed of the FSM for $\gamma$ from 0.1 to 45.1° in 1° steps.

We base the minimum value of the proposed range for the divergence angle on the maximum angular speed of a commercial FSM. This maximum angular speed dictates the minimum divergence angle of the proposed range when the tilt angle of the beam is 45° or larger [19]. Therefore, we propose to use the smallest divergence angle in the proposed range, 0.07°, to keep the needed angular speed within the range of a commercial FSM.

**Vibration Effect.** Possible motions of the train are modeled in three dimensions: longitudinal; along the direction in which the train moves, vertical, and lateral. Figure 7 shows these directions in reference to the train position. Because the train smoothly moves in the longitudinal direction, we analyze the vibration in the vertical and lateral directions.

*a) Vertical train vibration:* We first investigate the impact of the vertical displacement of the train on the received power to determine the maximum amplitude of the vertical displacement that may cause connectivity problems between a BS and the train. Figure 8 shows how the received power changes as the vertical displacement of the train varies between 0 and 60 mm. As the figure shows, there is a drastic reduction in the received power with the increase in the vertical displacement of the train for the narrow beam. Specifically, the narrow beam crosses the receiver sensitivity threshold when the amplitude of the vertical displacement of the train equals to 39 mm. The loss of received power in this figure occurs because the detector decoupling loss of the narrow beam becomes severe. However, the changes in the received power of the considered wide beam modalities are too small to measure. Moreover, among the wide beams presented in Figure 8, the ones in the proposed divergence-angle range provide a received power greater than the receiver sensitivity threshold when the extent of the maximum vertical displacement changes from 0 to 60 mm.

In the remainder of this paper, we use 30 and 50 mm as the two amplitudes of vertical displacement that yield the received power values above and below the receiver sensitivity threshold for the narrow beam, respectively. By doing so, we

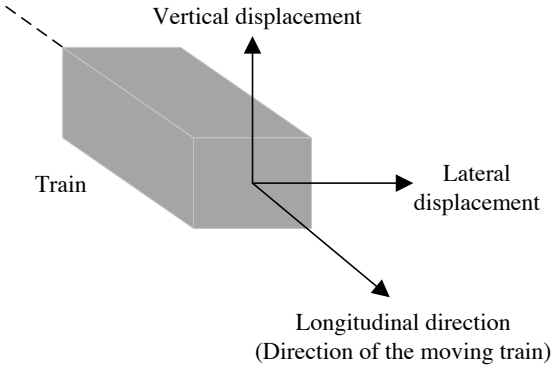


Fig. 7. 3-dimensional view of the train and the vibration types.

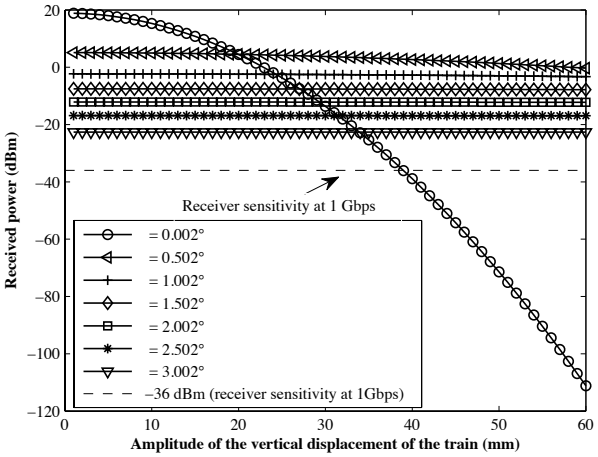


Fig. 8. Received power in function of the amplitude of vertical displacement of the train.

adopt a vertical displacement (i.e., 30 mm) that does not cause a disconnection and a vertical displacement (i.e., 50 mm) that may cause a disconnection between a BS and the train.

We consider that the vertical displacement of the train can be positive (i.e., upwards) or negative (i.e., downwards). Figure 9 depicts the scenarios for positive or negative vertical displacement of the train. This vertical vibration is modeled as sinusoids, as Figures 10 and 11 show. The sinusoidal vibrations can be generated by the unevenness of a wheel of an HST or the rail [68]. These figures show the vertical displacement of an HST traveling at 300 km/h. We sample 100 data points of the displacement produced by vertical vibration over a 1 second-window to be used as the extent and the direction of the vibration and mark them in these figures. The vibrational frequency in this analysis was set to 80 Hz, which is the upper frequency limit of the ground vibration measured when a HST travels at speeds up to 290 km/h [27].

Figures 12 and 13 show the corresponding impact of the train vibration on the received power for maximum vertical displacements of 30mm and 50mm, respectively. When the

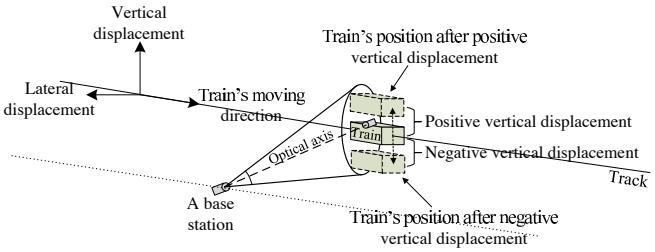


Fig. 9. A scenario for positive or negative vertical displacement of the train.

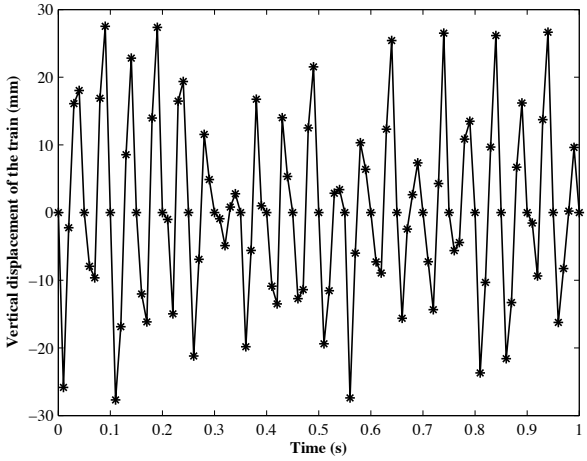


Fig. 10. Vertical displacement model of an HST with a maximum amplitude of 30 mm and a frequency of 80 Hz during a 1 second time window.

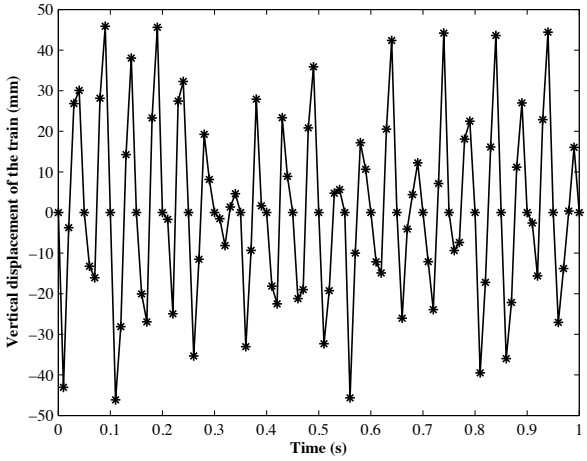


Fig. 11. Vertical displacement model of an HST with a maximum amplitude of 50 mm and a frequency of 80 Hz during a 1 second time window.

vertical displacement of the train fluctuates, the received power of the narrow beam also fluctuates. The 50 mm displacement causes the received power to decrease below the the receiver sensitivity threshold because the center of the beam moves far from the receiver, and the received power decreases in accordance with the gaussian distribution of the beam. Therefore, a vertical displacement of 50 mm may result in disconnections between the BS and the receiver on the train. These results

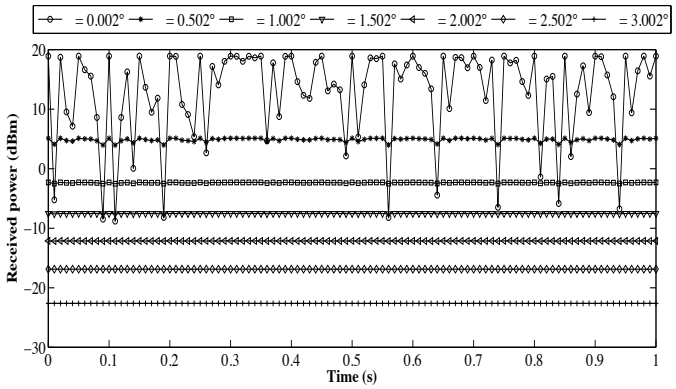


Fig. 12. The impact of the vertical vibration of the train with a frequency of 80 Hz and a maximum displacement of 30 mm on the received power for 1 second.

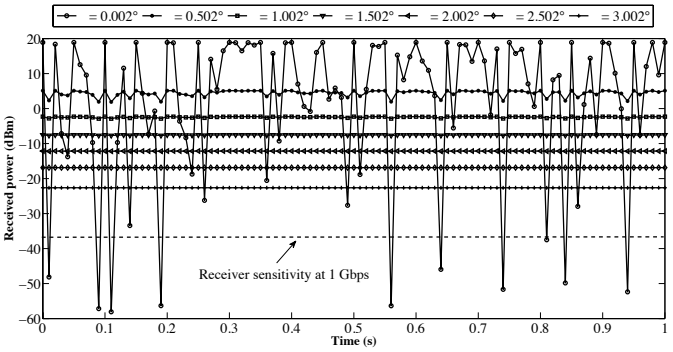


Fig. 13. The impact of the vertical vibration of the train with a frequency of 80 Hz and a maximum displacement of 50 mm for 1 second on the received power.

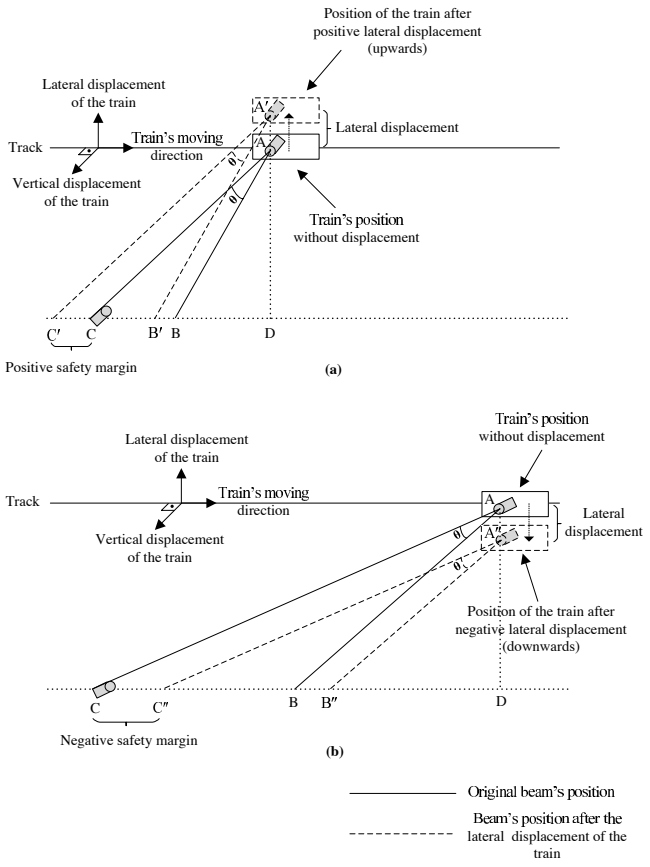


Fig. 14. Top views of **(a)** a the positive (updwards) lateral displacement of the train and the corresponding safety margin, $[C'C]$, on the covered distance, and **(b)** a negative (downwards) lateral displacement of the train and the corresponding safety margin, $[CC"]$.

show that a narrow beam may not be an appropriate beam modality for ground-to-train FSO communications for HSTs undergoing vertical displacements of 50 mm and larger. Moreover, Figures 12 and 13 show that the divergence angles in the proposed range yield a received power above the receiver sensitivity threshold for a vertical displacement of the train of up to 50 mm.

*b) Lateral train vibration:* In addition to vertical displacement of the train, we investigate the impact of lateral displacement of the train for train-to-ground traffic. We calculate the coverage-distance safety margins that guarantee a BS to be covered by the transmitting beam from the train in case of a lateral displacement of the train for each of the considered divergence angles. We use the largest coverage distance along the track for each of these angles. As the boundary of a covered distance is limited by the divergence angle, we consider that a reliable coverage distance is the largest one for each divergence angle minus the safety margins needed for compensating the largest lateral displacement caused by lateral vibration. These safety margins might be required at the coverage boundaries of the transmitting beam not to lose the line-of-sight between the train and a BS when a lateral displacement occurs on the train. We consider $d_2$ = 15 m as the starting position where the train and a BS make contact for the first time. This position is found at the leftmost position of the coverage distance of train's transmitter [3]. The rightmost position covered by the beam corresponds to the maximum achievable distance of the beam. Figure 14 depicts the two possible lateral displacements (i.e., upwards or downwards) of the train, and the corresponding safety margins, respectively. $[C'C]$ and $[CC'']$ in Figures 14(a) and 14(b) show the safety margins for positive and negative lateral displacement of the train, respectively. Table IV shows these values for sampled divergence angles. For the considered divergence angles, the positive safety margin at the leftmost coverage point is calculated using triangle similarity between the $A'C'D$ and $ACD$ triangles in Figure 14(a). Because we use a positive lateral displacement of 50 mm, $\frac{|A'A|}{|A'D|} = \frac{|C'C|}{|C'D|}$, where $|A'A| = 0.05$ m, yields a 0.75 m displacement on the left edge of the covered distance along the parallel line that BSes are located in Figure 14(a). Similarly, the negative safety margin at the rightmost coverage point in Figure 14(b) is calculated considering the maximum achievable distance and the triangle similarity between the $ACD$ and $A''C''D$ triangles in Figure 14(b), where $\frac{|AA''|}{|AD|} = \frac{|CC''|}{|CD|}$ and $|A'A| = 0.05$ m, for all considered divergence angles. Furthermore, considering the maximum achievable distance of a beam in the proposed range of divergence angles, a negative lateral displacement (in the downwards direction) of the train causes the maximum

coverage point of the 0.07° beam to be adjusted to 4,931 m, which yields a 259-m safety margin. In other words, a 50-mm lateral displacement of the train would leave 259 m of the coverage length uncovered when the divergence angle is selected as 0.07°. Therefore, we exclude that length from the maximum achievable distance. Similarly, the same negative lateral displacement causes the beam with a divergence angle of 2.002° to displace about 9 meters. Therefore, a lateral displacement of 50 mm defines safety margins (i.e., 0.75 and [9, 259] m, respectively) for the beams in the proposed range such that the train and corresponding BS keep line-of-sight despite the occurrence of lateral vibrations.

### A. Experimental Results

We performed a laser experiment in a laboratory environment to show that the theoretical received power values in (5) match actual power values. The experiment consists of measuring the received power at different distances using an optical power meter. The transmitter comprises a collimated 532-nm laser diode with an output power of 70 mW and a biconvex lens with a focal length of 10 cm to diverge the beam. The receiver is a bolometer (Scientech 361) with an aperture size of 2.5 cm. We measured the received power and the beam diameter for different distances between the transmitter and the receiver. The considered distances are from 10 to 25 meters. The longest considered distance is limited by the sensitivity of the bolometer. Figure 15 shows the bolomoter used in the experiment and the beam formation at the receiver when the light source is placed 20 meters away from the receiver. The laser beam through the lens sets a divergence angle of 10.5 mrad or 0.6°, as defined by:

$$\theta = 2 \arctan \left| \frac{D_{i+1} - D_i}{l} \right| \tag{7}$$

where $D_i$ and $D_{i+1}$ are the beam diameters at two separate points, $i$ and $i+1$, and $l$ is the distance between these two measurement points. The theoretical received power for each distance in the experiments is calculated by using (2), (5), (6), and (7). Figure 16 shows the comparison of the theoretical and experimental received power of the wide beam with a divergence angle of 0.6°. The results show that the experimental received power closely follows the theoretical model. It is worth nothing that the small discrepancies in the comparison may be caused by some measurement errors as exact measurement of spot diameter and power are complex. The results are encouraging.

We calculated the SNR and the BER using the received power values collected from the conducted experiment. The SNR at the receiver is given by [58], as:

$$SNR = \frac{RP_{rx}}{\sigma^2_{total}} \tag{8}$$

where $R$ is the responsivity of the photodiode in A/W, and $\sigma^2_{total}$ is the total noise variance, which is equal to the sum of the variances of shot, thermal, and background noises [50], [69]. The BER is expressed as:

$$BER = Q\left(\sqrt{SNR}\right) \tag{9}$$

where the Q function is the tail probability of the standard normal distribution and it is given as:

$$Q(x) = \frac{1}{2\pi} \int_x^\infty e^{\left(-y^2/(2)\right)} dy \tag{10}$$

We assumed an Si APD with a responsivity of 0.5 A/W being used for a system operating at 850 nm [70]. We also assumed that the total noise power in the system is equal to 10 $\mu$W [3], [71], [72]. The calculated BER for the received power values given in Figure 16 are negligibly small to provide an error-free transmission at 1 Gbps. This is an expected result because of the high transmission power the employed laser in the experiment. According to the calculated BER, a high-speed FSO communications system with a received power of greater than or equal to 77.5 $\mu$W can support an error-free transmission at 1 Gbps for the parameters used in this experiment.

Some other laboratory experiments for ground-to-train FSO communications, which use the same propagation model as (5), have been reported [35], [73]. These experiments achieved successful FSO communication between a toy train and a BS. By using a light source with an output power of 10 mW, a BER of $10^{-12}$ at 10 Mbps [73] and a data rate of 155 Mbps [35] are achieved, respectively. In another experiment, a diverged beam is used to show how the received power changes when the distance between the light source and the diverging lens varies [74]. The experimental results in [74] shows that a data rate of 622.08 Mbps is achieved when the minimum received power is -36 dBm. These experimental results support that the propagation model used in this paper is valid and matches the theocratical analysis.

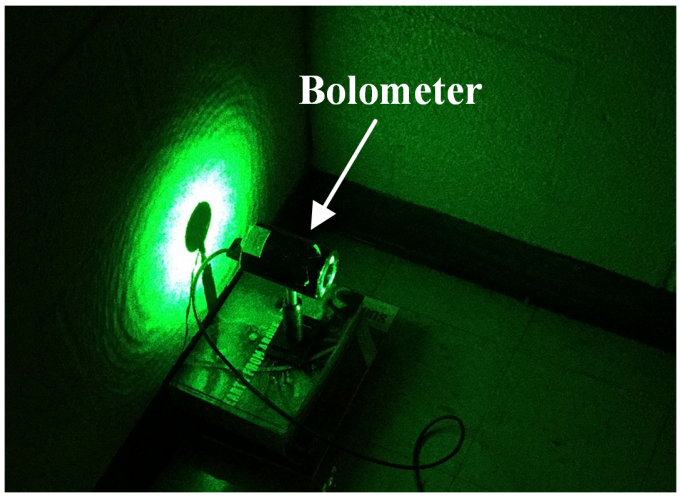


Fig. 15. The bolomoter used to measure the received power and the beam formation of the performed experiments.

## VI. Conclusions

We investigated two different laser beam modalities, narrow and wide beams, for free-space optical communications in the context of ground-to-train HST communications. We compared two beam modalities and revealed their advantages

TABLE IV
SAMPLED SAFETY MARGINS REQUIRED FOR DIFFERENT DIVERGENCE ANGLES TO COMPENSATE FOR LATERAL TRAIN VIBRATION.

| $\theta$ (degrees) | Safety Margin (m) |
|---|---|
| 0.002 | 9084.86 |
| 0.07 | 259 |
| 0.502 | 35.96 |
| 1.002 | 17.90 |
| 1.502 | 11.98 |
| 2.002 | 9.05 |
| 2.502 | 7.09 |
| 3.002 | 5.87 |

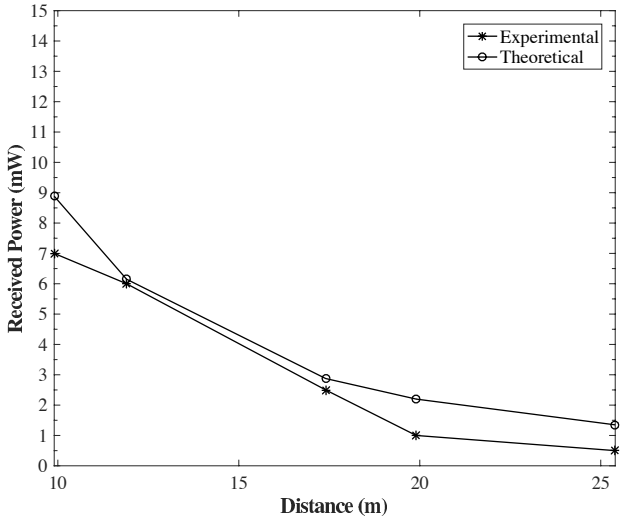


Fig. 16. The comparison of the experimental and the theoretical received power for the wide beam with a divergence angle of 0.6°.

and disadvantages. We also estimated the covered distance, steering speed, steering arc, covered area, and the impact of vibration for each angle. Considering the results presented in this paper, we propose to use a divergence-angle range to enable a contact time larger than or equal to the worst-case handover time. The impact of the vibration is also examined and our results show that the proposed range of divergence angles guarantees that the received power is larger than the receiver sensitivity threshold with the maximum vertical vibration amplitude smaller than or equal to 50 mm.

## ACKNOWLEDGMENT

We would like to thank Prof. Haim Grebel for gracefully allowing us to use his laboratory equipment to perform the reported laser experiment.

## REFERENCES

[1] G. Ollivier, R. Bullock, Y. Jing, J. Sondhri, N. Zhou, and World Bank Beijing. (2015, February) Chinese high-speed: an evaluation of traffic. [Online]. Available: http://www.railjournal.com/index.php/high-speed/chinese-high-speed-an-evaluation-of-traffic.html

[2] K. Mori, M. Terada, K. Nakamura, R. Murakami, K. Kaneko, F. Teraoka, D. Yamaguchi, and S. Haruyama, "Fast handover mechanism for high data rate ground-to-train free-space optical communication system," in *Globecom Workshops (GC Wkshps), 2014*, 2014, pp. 499–504.

[3] R. Paudel, Z. Ghassemlooy, H. Le-Minh, and S. Rajbhandari, "Modelling of free space optical link for ground-to-train communications using a gaussian source," *Optoelectronics, IET*, vol. 7, no. 1, pp. 1–8, 2013.

[4] T. Yuge and S. Sasaki, "Train radio system using leaky coaxial cable," in *Vehicular Technology Conference, 1984. 34th IEEE*, vol. 34. IEEE, 1984, pp. 43–48.

[5] M. Aguado, O. Onandi, P. Agustin, M. Higuero, and E. Taquet, "Wimax on rails," *IEEE Vehicular Technology Magazine*, vol. 3, no. 3, pp. 47–56, 2008.

[6] J. Conti, "High speeds at high speed," *Engineering & Technology*, vol. 4, no. 15, pp. 69–71, 2009.

[7] D. T. Fokum and V. S. Frost, "A survey on methods for broadband internet access on trains," *Communications Surveys & Tutorials, IEEE*, vol. 12, no. 2, pp. 171–185, 2010.

[8] A. Sniady and J. Soler, "Lte for railways: impact on performance of etcs railway signaling," *Vehicular Technology Magazine, IEEE*, vol. 9, no. 2, pp. 69–77, 2014.

[9] I. Ahmad and D. Habibi, "A novel mobile wimax solution for higher throughput," in *Networks, 2008. ICON 2008. 16th IEEE International Conference on*. IEEE, 2008, pp. 1–5.

[10] A. G. Alkholidi and K. S. Altowij, "Free space optical communication-stheory and practices," 2014.

[11] H. Urabe, S. Haruyama, T. Shogenji, S. Ishikawa, M. Hiruta, F. Teraoka, T. Arita, H. Matsubara, and S. Nakagawa, "High data rate ground-to-train free-space optical communication system," *Optical Engineering*, vol. 51, no. 3, pp. 031 204–1, 2012.

[12] S. Bloom, E. Korevaar, J. Schuster, and H. Willebrand, "Understanding the performance of free-space optics [invited]," *Journal of optical Networking*, vol. 2, no. 6, pp. 178–200, 2003.

[13] R. Kern and U. Kugel, "Pointing, acquisition and tracking (pat) subsystems and components for optical space communication systems," in *1989 Intl Congress on Optical Science and Engineering*. International Society for Optics and Photonics, 1989, pp. 97–107.

[14] J. He, R. A. Norwood, M. Brandt-Pearce, I. B. Djordjevic, M. Cvijetic, S. Subramaniam, R. Himmelhuber, C. Reynolds, P. Blanche, B. Lynn *et al.*, "A survey on recent advances in optical communications," *Computers & Electrical Engineering*, vol. 40, no. 1, pp. 216–240, 2014.

[15] B. H. Walke, S. Mangold, and L. Berlemann, *IEEE 802 wireless systems: protocols, multi-hop mesh/relaying, performance and spectrum coexistence*. John Wiley & Sons, 2007.

[16] Y. Zhou and B. Ai, "Handover schemes and algorithms of high-speed mobile environment: A survey," *Computer Communications*, vol. 47, pp. 1–15, 2014.

[17] W. Luo, R. Zhang, and X. Fang, "A comp soft handover scheme for lte systems in high speed railway," *EURASIP Journal on wireless Communications and Networking*, vol. 2012, no. 1, pp. 1–9, 2012.

[18] L. Zhu, F. R. Yu, and B. Ning, "A seamless handoff scheme for train-ground communication systems in cbtc," in *Vehicular Technology Conference Fall (VTC 2010-Fall), 2010 IEEE 72nd*. IEEE, 2010, pp. 1–5.

[19] Appliead Technology Associates (ATA). Fast Steering Mirrors (FSM) Overview. [Online]. Available: http://www.aptec.com/fast_steering_mirror.html

[20] Specifications of Fast Steering Mirrors (FSM Series). Newport Optical Solutions. [Online]. Available: http://www.newport.com/Fast-Steering-Mirrors/847119/1033/info.aspx#tab_Specifications

[21] High speed piezo steering mirrors 6-axis optical alignment platforms. PI. [Online]. Available: http://www.pi-usa.us/pdf/PI_Steering_Mirrors_High_and_Low_Bandwidth.pdf

[22] T. Arita and F. Teraoka, "Providing a high-speed train with a broadband nemo environment: a report of a field test using a train in service," in *Proceedings of the Sixth Asian Internet Engineering Conference*. ACM, 2010, pp. 64–71.

[23] D. Killinger, "Free space optics for laser communication through the air," *Optics and Photonics News*, vol. 13, no. 10, pp. 36–42, 2002.

[24] Z. Ghassemlooy and W. Popoola, *Terrestrial free-space optical communications*. INTECH Open Access Publisher, 2010.

[25] B. Glushko, D. Kin, and A. Shar, "Gigabit optical wireless communication system for personal area networking," *Optical Memory and Neural Networks*, vol. 22, no. 2, pp. 73–80, 2013.

[26] H. Kaushal and G. Kaddoum, "Free space optical communication: Challenges and mitigation techniques," *arXiv preprint arXiv:1506.04836*, 2015.

[27] W. Zhai, Z. He, and X. Song, "Prediction of high-speed train induced ground vibration based on train-track-ground system model," *Earthquake Engineering and Engineering Vibration*, vol. 9, no. 4, pp. 545–554, 2010.

[28] T.-H. Ho, S. Trisno, A. Desai, J. Llorca, S. D. Milner, and C. C. Davis, "Performance and analysis of reconfigurable hybrid fso/rf wireless networks," in *Lasers and Applications in Science and Engineering*. International Society for Optics and Photonics, 2005, pp. 119–130.

[29] J. Rzasa, M. C. Ertem, and C. C. Davis, "Pointing, acquisition, and tracking considerations for mobile directional wireless communications systems," in *SPIE Optical Engineering+ Applications*. International Society for Optics and Photonics, 2013, pp. 88 740C–88 740C.

[30] D. K. Borah, A. C. Boucouvalas, C. C. Davis, S. Hranilovic, and K. Yiannopoulos, "A review of communication-oriented optical wireless systems," *EURASIP Journal on Wireless Communications and Networking*, vol. 2012, no. 1, pp. 1–28, 2012.

[31] V. V. Nikulin, J. Sofka, and R. M. Khandekar, "Effect of the sampling rate of the tracking system on free-space laser communications," *Optical Engineering*, vol. 47, no. 3, pp. 036 003–036 003, 2008.

[32] G. A. Cap, H. H. Refai, and J. J. Sluss Jr, "Optical tracking and auto-alignment transceiver system," *Aerospace and Electronic Systems Magazine, IEEE*, vol. 25, no. 9, pp. 26–34, 2010.

[33] A. A. Portillo, G. G. Ortiz, and C. Racho, "Fine pointing control for optical communications," in *Aerospace Conference, 2001, IEEE Proceedings.*, vol. 3. IEEE, 2001, pp. 3–1541.

[34] H. Kotake, S. Haruyama, and M. Nakagawa, "A New Ground-to-Train Communication System Using Free-Space Optics Technology," *IEEJ Transactions on Industry Applications*, vol. 128, pp. 523–528, 2008.

[35] R. Paudel, H. Le Minh, Z. Ghassemlooy, M. Iaz, and S. Rajbhandari, "High speed train communications systems using free space optics," 2010.

[36] T. C. Shen, R. J. Drost, C. C. Davis, and B. M. Sadler, "Design of dual-link (wide-and narrow-beam) led communication systems," *Optics express*, vol. 22, no. 9, pp. 11 107–11 118, 2014.

[37] B. Woodward, *Fiber Optics Installer (FOI) Certification Exam Guide*. John Wiley & Sons, 2014.

[38] P. F. Goldsmith, I. of Electrical, E. Engineers, M. Theory, and T. Society, *Quasioptical systems: Gaussian beam quasioptical propagation and applications*. IEEE press New York, 1998.

[39] J. Alda, "Laser and gaussian beam propagation and transformation," *Encyclopedia of optical engineering*, pp. 999–1013, 2003.

[40] Fiber optic network optical wavelength transmission bands. Last access: 4/10/2016. [Online]. Available: http://www.thefoa.org/tech/ref/basic/SMbands.html

[41] Optical fiber communications. Last access: 4/10/2016. [Online]. Available: https://goo.gl/ACvTZi

[42] L. Gasca. (2008, Jun.) From o to l: The future of optical-wavelength bands. Broadband Communities. Last Access: 4/10/2016. [Online]. Available: http://goo.gl/F8GBQq

[43] Fiber-to-Fiber Media Converter Overview. Omnitron Systems. Last access: 9/30/2016. [Online]. Available: https://goo.gl/05AfQR

[44] Fiber media converters. Perle Inc. Last access: 9/30/2016. [Online]. Available: https://goo.gl/EcKWvq

[45] Singlemode - multimode converter. Fiberbit Technology Co. Ltd. Last access: 9/30/2016. [Online]. Available: https://goo.gl/Kfpaz9

[46] D. C. Brien, G. Faulkner, H. Le Minh, O. Bouchet, M. El Tabach, M. Wolf, J. W. Walewski, S. Randel, S. Nerreter, M. Franke *et al.*, "Gigabit optical wireless for a home access network," in *Personal, Indoor and Mobile Radio Communications, 2009 IEEE 20th International Symposium on*. IEEE, 2009, pp. 1–5.

[47] B. Bova, *The Story of Light*. Sourcebooks, Inc., 2002.

[48] A. L. H. Laser-Radio. LightPointe. [Online]. Available: http://www.lightpointe.com/airebridge-lx-1.html

[49] D. V. Hahn, D. M. Brown, A. M. Brown, C.-H. Bair, M. J. Mayr, N. W. Rolander, J. E. Sluz, and R. Venkat, "Conformal free-space optical communications terminal designs for highly confined vehicles," *Johns Hopkins APL technical digest*, vol. 30, no. 4, pp. 321–330, 2012.

[50] A. K. Majumdar and J. C. Ricklin, *Free-space laser communications: principles and advances*. Springer Science & Business Media, 2010, vol. 2.

[51] MATLAB, *version 8.3.0.532 (R2014a)*. Natick, Massachusetts: The MathWorks Inc., 2014.

[52] M. Yoshikawa, A. Murakami, J. Sakurai, H. Nakayama, and T. Nakamura, "High power vcsel devices for free space optical communications," in *Electronic Components and Technology Conference, 2005. Proceedings. 55th*. IEEE, 2005, pp. 1353–1358.

[53] H. Le Minh, D. O'Brien, and G. Faulkner, "A gigabit/s indoor optical wireless system for home access networks," in *Communication Systems Networks and Digital Signal Processing (CSNDSP), 2010 7th International Symposium on*. IEEE, 2010, pp. 532–536.

[54] H. Le Minh, Z. Ghassemlooy, D. O'Brien, and G. Faulkner, "Indoor gigabit optical wireless communications: challenges and possibilities," 2010.

[55] C. Oh, F. Huijskens, Z. Cao, E. Tangdiongga, and A. Koonen, "Toward multi-gbps indoor optical wireless multicasting system employing passive diffractive optics," *Optics letters*, vol. 39, no. 9, pp. 2622–2625, 2014.

[56] C. Oh, E. Tangdiongga, and A. Koonen, "Steerable pencil beams for multi-gbps indoor optical wireless communication," *Optics letters*, vol. 39, no. 18, pp. 5427–5430, 2014.

[57] D. C. OBrien, M. Katz, P. Wang, K. Kalliojarvi, S. Arnon, M. Matsumoto, R. Green, and S. Jivkova, "Short-range optical wireless communications," in *Wireless world research forum*, 2005, pp. 1–22.

[58] J. M. Kahn and J. R. Barry, "Wireless infrared communications," *Proceedings of the IEEE*, vol. 85, no. 2, pp. 265–298, 1997.

[59] T. Cevik and S. Yilmaz, "An overview of visible light communication systems," *arXiv preprint arXiv:1512.03568*, 2015.

[60] Fundamentals of power and energy measurement. Introduction to laser beam and spectral measurements. Last access: 4/21/2016. [Online]. Available: http://www.astro.caltech.edu/~lah/ay105/pdf/e1-photodiode.pdf

[61] J. Ready, "Optical detectors and human vision," *Fundamentals of photonics*, p. 219, 1991.

[62] Si photodiodes. Hamamatsu Corp. Last Access: 4/25/2016. [Online]. Available: http://www.hamamatsu.com/us/en/product/category/3100/4001/4103/index.html

[63] Compound semiconductor photosensors. Hamamatsu Corp. Last access: 4/27/2016. [Online]. Available: https://goo.gl/w65E3q

[64] Optical & ic selector guide. Semtech. Last access: 4/27/2016. [Online]. Available: http://www.semtech.com/images/mediacenter/collateral/opticalsg.pdf

[65] Large area Si PIN photodiodes, s3204/s3584 series. Hamamatsu Corp. Last Access: 4/28/2016. [Online]. Available: https://goo.gl/Tg7UIo

[66] Optical components. Finisar Corp. Last Access: 4/29/2016. [Online]. Available: https://goo.gl/MRL0jG

[67] InGaAs photodiodes with preamp, ROSA type, G12072-54. Hamamatsu Corp. Last Access: 5/1/2016. [Online]. Available: https://goo.gl/fXWr2q

[68] D. Thompson, *Railway noise and vibration: mechanisms, modelling and means of control*. Elsevier, 2008.

[69] H. Manor and S. Arnon, "Performance of an optical wireless communication system as a function of wavelength," *Applied optics*, vol. 42, no. 21, pp. 4285–4294, 2003.

[70] The datasheet for s12023 series si apd. Hamamatsu Corp. Last access: 1/26/2017. [Online]. Available: https://goo.gl/TcNF8k

[71] G.-y. Hu, C.-y. Chen, and Z.-q. Chen, "Free-space optical communication using visible light," *Journal of Zhejiang University-SCIENCE A*, vol. 8, no. 2, pp. 186–191, 2007.
[72] M.-A. Khalighi, F. Xu, Y. Jaafar, and S. Bourennane, "Double-laser differential signaling for reducing the effect of background radiation in free-space optical systems," *Journal of Optical Communications and Networking*, vol. 3, no. 2, pp. 145–154, 2011.
[73] R. Paudel, Z. Ghassemlooy, H. Le-Minh, S. Rajbhandari, and B. Livingstone, "Investigation of fso ground-to-train communications in a laboratory environment," in *2011 Second Asian Himalayas International Conference on Internet (AH-ICI)*. IEEE, 2011.
[74] D. Zhou, P. G. LoPresti, and H. H. Refai, "Enlargement of beam coverage in fso mobile network," *Journal of Lightwave Technology*, vol. 29, no. 10, pp. 1583–1589, 2011.

**Yagiz Kaymak** received his B.S. degree in Mathematics from Celal Bayar University, Turkey, in 2003 and his M.S. degree in Computer Science from Ege University, Turkey, in 2011. He is currently working toward the Ph.D. degree in Computer Engineering at New Jersey Institute of Technology (NJIT), Newark, NJ, USA. He is a teaching assistant and a member of Networking Research Laboratory in the Department of Electrical and Computer Engineering, NJIT. His research interests include free-space optical communication for high-speed trains, data center networking, peer-to-peer video streaming and distributed systems.

**Roberto Rojas-Cessa** (S'97-M'01-SM'11) received the Ph.D. degree in Electrical Engineering from Polytechnic Polytechnic University (now the New York University Tandon School of Engineering, Polytechnic Institute), Brooklyn, NY. Currently, he is an Associate Professor in the Department of Electrical and Computer Engineering, New Jersey Institute of Technology. He has been involved in design of systems for high-speed computer communications, and in the development of high-performance and scalable packet switches and reliable switches. He participated in the design of a 40 Tb/s core router in Coree, Inc, in Tinton Falls, NJ. His research interests include data center networks, high-speed switching and routing, fault tolerance, quality-of-service networks, network measurements, and distributed systems. He was an Invited Fellow of the Japanese Society for the Advancement of Science in 2009. He visited the University of Electro-Communications, Japan. He was a Visiting Professor in Thammasat University, Thailand. He is a co-author of the book "Advanced Internet Protocols, Services, and Applications," Wiley and Sons, 2012. His research has been funded by U.S. National Science Foundation and private companies. He has served in technical committees for numerous IEEE conferences, as a reviewer for several IEEE journals, and as a reviewer and panelist for U.S. National Science Foundation and U.S. Department of Energy. He is the recipient of the Excellence in Teaching Award 2013 from the Newark College of Engineering. He is a recipient of New Jersey Inventors Hall of Fame - Innovators Award in 2013. He is a Senior Member of IEEE.

**Jianghua Feng** received his B.S. and M.S. degrees in Electric Machine and Control from Zhejiang University, Hangzhou, China respectively in 1986 and 1989 and his Ph.D. degree in Control Theory and Control Engineering from Central South University, Changsha, China in 2008. He joined CSR Zhuzhou Institute Co. Ltd., Zhuzhou, China in 1989. His research interest is electrical systems and their control in the field of rail transportation. He is now a professorate senior engineer and has a number of papers published in such journals and conferences as Proceedings of China Internet, IEEE International Symposium on Industrial Electronics, International Power Electronics and Motion Control Conference, and IEEE Conference on Industrial Electronics and Applications.

**Nirwan Ansari** (S'78-M'83-SM'94-F'09) is Distinguished Professor of Electrical and Computer Engineering at the New Jersey Institute of Technology (NJIT). He has also been a visiting (chair) professor at several universities such as High-level Visiting Scientist at Beijing University of Posts and Telecommunications. Professor Ansari is authoring Green Mobile Networks: A Networking Perspective (John Wiley, 2016) with T. Han, and co-authored two other books. He has also (co-)authored over 500 technical publications, over one third published in widely cited journals/magazines. He has guest-edited a number of special issues covering various emerging topics in communications and networking. He has served on the editorial/advisory board of over ten journals. Professor Ansari was elected to serve in the IEEE Communications Society (ComSoc) Board of Governors as a member-at-large, has chaired ComSoc technical committees, and has been actively organizing numerous IEEE International Conferences/Symposia/Workshops. He has frequently delivered keynote addresses, distinguished lectures, tutorials, and invited talks. Some of his recognitions include IEEE Fellow, several Excellence in Teaching Awards, a couple of best paper awards, the NCE Excellence in Research Award, the ComSoc AHSN TC Outstanding Service Recognition Award, the NJ Inventors Hall of Fame Inventor of the Year Award, the Thomas Alva Edison Patent Award, Purdue University Outstanding Electrical and Computer Engineer Award, and designation as a COMSOC Distinguished Lecturer. He has also been granted over 25 U.S. patents. He received a Ph.D. from Purdue University in 1988, an MSEE from the University of Michigan in 1983, and a BSEE (summa cum laude with a perfect GPA) from NJIT in 1982.

**MengChu Zhou** (S'88-M'90-SM'93-F'03) received his B.S. degree in Control Engineering from Nanjing University of Science and Technology, Nanjing, China in 1983, M.S. degree in Automatic Control from Beijing Institute of Technology, Beijing, China in 1986, and Ph. D. degree in Computer and Systems Engineering from Rensselaer Polytechnic Institute, Troy, NY in 1990. He joined New Jersey Institute of Technology (NJIT), Newark, NJ in 1990, and is now a Distinguished Professor of Electrical and Computer Engineering. His research interests are in Petri nets, Internet of Things, big data, web services, manufacturing, transportation, and energy systems. He has over 640 publications including 12 books, 320+ journal papers (240+ in IEEE Transactions), and 28 book-chapters. He is the founding Editor of IEEE Press Book Series on Systems Science and Engineering. He is a recipient of Humboldt Research Award for US Senior Scientists, Franklin V. Taylor Memorial Award and the Norbert Wiener Award from IEEE Systems, Man and Cybernetics Society. He is a life member of Chinese Association for Science and Technology-USA and served as its President in 1999. He is

a Fellow of International Federation of Automatic Control (IFAC) and American Association for the Advancement of Science (AAAS).